Vibrational assignments and conformer stability determination of cyclobutyldichlorosilane by variable temperature Raman spectra in krypton solution

Reference:

Deodhar Bhushan S., Brenner Reid E., Sawant Dattatray K., Guirgis Gamil A., Geboes Yannick, Herrebout Wouter, Durig James R..- Vibrational assignments and conformer stability determination of cyclobutyldichlorosilane by variable temperature Raman spectra in krypton solution

Vibrational spectroscopy - ISSN 0924-2031 - (2015), p. 1-39

Full text (Publishers DOI): http://dx.doi.org/doi:10.1016/j.vibspec.2015.10.009

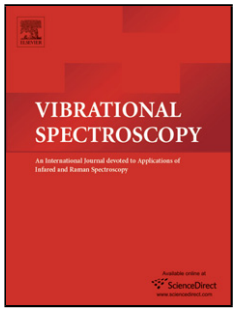

Title: Vibrational assignments and conformer stability determination of cyclobutyldichlorosilane by variable temperature Raman spectra in krypton solution

Author: Bhushan S. Deodhar Reid E. Brenner Dattatray K. Sawant Gamil A. Guirgis Yannick Geboes Wouter A. Herrebout James. R. Durig

PII: S0924-2031(15)30025-4
DOI: http://dx.doi.org/doi:10.1016/j.vibspec.2015.10.009
Reference: VIBSPE 2467

To appear in: *VIBSPE*

Received date: 21-7-2015
Revised date: 2-10-2015
Accepted date: 27-10-2015

Please cite this article as: Bhushan S.Deodhar, Reid E.Brenner, Dattatray K.Sawant, Gamil A.Guirgis, Yannick Geboes, Wouter A.Herrebout, James.R.Durig, Vibrational assignments and conformer stability determination of cyclobutyldichlorosilane by variable temperature Raman spectra in krypton solution, Vibrational Spectroscopy http://dx.doi.org/10.1016/j.vibspec.2015.10.009

Vibrational assignments and conformer stability determination of cyclobutyldichlorosilane by variable temperature Raman spectra in krypton solution

Bhushan S. Deodhar[a1], Reid E. Brenner[a1], Dattatray K. Sawant[a1], Gamil A. Guirgis[b], Yannick Geboes[c], Wouter A. Herrebout[c], James. R. Durig[a,*]

[a]Department of Chemistry, University of Missouri-Kansas City, Kansas City, MO 64110 USA

[b] Department of Chemistry and Biochemistry, College of Charleston, Charleston, SC 29424, USA

[c]Department of Chemistry, Universitair Centrum Antwerpen, 171 Groenenborglaan, Antwerpen 2020, Belgium

[*]Corresponding author, phone: 01 816-235-6038, fax: 01 816-235-2290, email: durigj@umkc.edu

[1]Taken in part from the dissertations of B.S. Deodhar, R.E. Brenner, and D.K. Sawant which will be submitted in partial fulfillment of their Ph.D. degrees.

Highlights

- Complete vibrational assignment has been obtained for cyclobutyldichlorosilane.
- Enthalpy difference has been determined between the four forms.
- Ab initio calculations were performed for the four conformers.

Abstract: The infrared spectra (3100 to 300 cm^{-1}) in the gas phase and Raman spectra (3100 to 150 cm^{-1}) of the liquid of cyclobutyldichlorosilane (c-$C_4H_7SiHCl_2$) have been recorded. Variable temperature (-143°C to -123°C) studies of the Raman spectra (3100 to 300 cm^{-1}) dissolved in liquid krypton have been carried out. From these data, the experimental stabilities of the conformer have been determined to be Eq-g > Ax-t > Eq-t >Ax-g. The enthalpy difference between Eq-g and Ax-t has been determined from band pairs to be 85 ± 10 cm^{-1} (1.01 ± 0.11 kJ mol^{-1}) with the Eq-g conformer the more stable form. The enthalpy difference between Eq-g and Eq-t is 116 ± 43 cm^{-1} (1.39 ± 0.52 kJ mol^{-1}) and the enthalpy difference between Eq-g and Ax-g has been determined to be 138 ± 42 cm^{-1} (1.66 ± 0.51 kJ mol^{-1}) with the Eq-g conformer as the more stable form. The percentage of the equatorial gauche conformer is estimated to be 47% at ambient temperature. To support the spectroscopic study, ab initio calculations by the Møller-Plesset perturbation method to second order MP2 (full) and density functional theory calculations by the B3LYP method have been carried out. The infrared intensities, Raman activities, vibrational frequencies and band contours have been predicted from MP2 (full)/6-31G(d) calculations and these theoretical values are compared to the experimental ones when available. The conformational stabilities have been predicted from theoretical calculations with basis sets up to 6-311+G(2d,2p) from both MP2(full) and density functional theory calculations by the B3LYP method. The results are discussed and compared to the corresponding properties of some related molecules.

Keywords: Cyclobutyldichlorosilane; Raman; Krypton; Conformer stability; Ab intio calculations

1. Introduction

The structural nature of organic rings called into question whether molecules such as cyclobutane were planar or puckered. Initial investigations[1–3] showed that the structure of cyclobutane was indeed puckered and the planar conformation was determined to be a higher energy state. The addition of monosubstituted groups (halides and silane) into cyclobutane as a consequence adds more complexity for determination of molecular structure. The complexity is the result of different conformational structures (conformers) for each molecule.

Initial vibrational studies for bromocyclobutane [4–6], chlorocyclobutane [4,6–9], and cyanocyclobutane [6] showed evidence of the equatorial conformer for each molecule as the most stable conformer. Additionally, cyclobutylsilane [10,11] was also investigated by similar methods and reported the existence of two puckered conformers with the more stable form having the silicon atom in the equatorial position.

The purpose of this research is to expand on the knowledge of monosubstituted cyclobutane molecules by performing a fundamental investigation of the cyclobutyldichlorosilane molecule and reporting our results. The information obtained from this investigation will help to establish a more accurate relationship between conformational stability and cyclobutylsilane derivatives.

We previously performed an initial investigation of the title compound [12]. The IR spectrum of the gas (3100 to 300 cm^{-1}) and Raman spectrum of the liquid (3100 to 150 cm^{-1}) were reported. Additionally ab initio calculations using MP2 and B3LYP methods were carried out. Vibrational frequencies, infrared intensities, Raman activities, and band contours were reported. The calculations predicted the conformational stability (Eq-t > Eq-g > Ax-t > Ax-g) with Eq-t conformer being the most stable. The previous study did not contain sufficient experimental data to present a thorough vibrational assignment. Additionally the potential energy distribution (PED) for the percent contribution of each vibration mode to the vibrational frequency was not given. Lastly there was no experimental determination of conformational stability for cyclobutydichlorosilane.

This investigation reports additional new scientific information for cyclobutyldichlorosilane. Using the predictions from our previous work, we now present a more thorough vibrational assignment by reporting an expanded Raman spectrum of the liquid and recorded the Raman spectrum in krypton solution. From ab initio calculation and variable

temperature Raman spectra in krypton solution, a new determination of conformational stability of cyclobutyldichlorosilane's four conformers (Fig. 1) has been given.

The variable temperature Raman spectra (3100 to 300 cm^{-1}) from -143°C to -123°C of cyclobutyldichlorosilane dissolved in krypton solution are reported along with the expanded Raman spectrum (3100 to 150 cm^{-1}) of the liquid. A comprehensive vibrational assignment table has been made using the Raman spectra in the liquid phase, Raman spectra of the molecule dissolved in Krypton solution, and previously reported IR spectrum of the gas. The enthalpy differences between the four conformers have been determined using the temperature dependent Raman spectra in krypton solution. The conformational stability has been made for the molecule's four conformers. The results of these spectroscopic, structural, and theoretical studies of cyclobutyldichlorosilane are reported herein.

2. Experimental methods

The sample of cyclobutyldichlorosilane was prepared by coupling trichlorosilane to the Grignard reagent of cyclobutyl magnesium bromide in dry diethyl ether under dry nitrogen. After stirring over night at room temperature the sample was filtered under nitrogen and the ether was distilled off. The product was originally purified by trap-to-trap distillation twice and the final purification was obtained at low pressure and low temperature by a sublimation column. The sample was further purified by a fractionation column and the purity of the sample was verified from the infrared spectra of the gas and NMR spectrum of the liquid. The pure sample exists as a liquid under ambient conditions.

The mid-infrared spectrum of the gas (Fig. 2A) was obtained from 3100 to 300 cm^{-1} on a Perkin-Elmer model 2000 Fourier transform spectrometer equipped with a Ge/CsI beamsplitter and a DTGS detector. Atmospheric water vapor was removed from the spectrometer housing by purging with dry nitrogen. The spectrum of the gas was obtained with a theoretical resolution of 0.5 cm^{-1} for the gas and 2 cm^{-1} for the solid with 128 interferograms added and truncated.

The Raman spectrum of the liquid (Fig. 3A) was recorded on a Spex model 1403 spectrophotometer equipped with a Spectra-Physics model 2017 argon ion laser operating on the 514.5 nm line. The laser power used was 1.5 W with a spectral bandpass of 3 cm^{-1}. The spectrum of the liquid was recorded with the sample sealed in a Pyrex glass capillary. The measurements of

the Raman frequencies are expected to be accurate to ± 2 cm^{-1}. All of the observed bands in the Raman spectra of the liquid along with their proposed assignments are listed in Tables 1, 2, 3 and 4.

The Raman spectra of the sample dissolved in liquefied krypton (Fig. 4) were recorded at three different temperatures (-143°C to -123°C) on a Trivista 557 spectrometer consisting of a double f = 50 cm monochromator equipped with a 2000 lines mm^{-1} grating, a f = 70 cm spectrograph equipped with a 2400 lines mm^{-1} grating, and a back-illuminated LN2-cooled PI Acton Spec-10:2 kB/LN 2048 x 512 pixel CCD detector. For all experiments, the 514.5 nm line of a 2017-Ar S/N 1665 Spectra-Physics argon ion laser was used for Raman excitation, with the power set to 0.8 W. Signals related to the plasma lines were removed by using an interference filter. The frequencies were calibrated using Neon emission lines and are expected to be accurate within 0.4 cm^{-1}. The experimental set-up used to investigate the solutions has been described previously [13–15]. A home-built liquid cell equipped with four quartz windows at right angles was used to record the spectra.

3. Theoretical methods

The ab initio calculations were performed with the Gaussian-03 program [16] using Gaussian-type basis functions. The energy minima with respect to nuclear coordinates were obtained by the simultaneous relaxation of all geometric parameters by using the gradient method of Pulay [17]. A variety of basis sets as well as the corresponding ones with diffuse functions were employed with the Møller-Plesset perturbation method [18] to the second order MP2 with full electron correlation as well as with the density functional theory by the B3LYP method. The predicted conformational energy differences are listed in Table 5.

In order to obtain descriptions of the molecular motions involved in the fundamental modes of cyclobutyldichlorosilane, a normal coordinate analysis was carried out. The force field in Cartesian coordinates was obtained with the Gaussian 03 program at the MP2(full) level with the 6-31G(d) basis set. By using the B matrix [19], the force field in Cartesian coordinates was converted to force constants in internal coordinates. Subsequently, 0.88 was used as the scaling factor for the CH stretches and deformations, and 0.90 was used for all other modes excluding the heavy atom bends to obtain the fixed scaled force constants and resultant wavenumbers. A set of symmetry coordinates was used (Table S1) to determine the corresponding potential energy

distributions (P.E.D.s). A comparison between the observed and calculated wavenumbers, along with the calculated infrared intensities, Raman activities, depolarization ratios and potential energy distributions for the Eq-t, Eq-g, Ax-t and Ax-g conformers of cyclobutyldichlorosilane are given in Tables 1-4 respectively. A, B and C type band contours [20] were predicted for all four conformers and are given in Tables 1-4 to assist with vibrational assignments.

The vibrational spectra were predicted from the MP2(full)/6-31G(d) calculations. The predicted scaled frequencies were used together with a Lorentzian function to obtain the simulated spectra. Infrared intensities were obtained based on the dipole moment derivatives with respect to Cartesian coordinates. The derivatives were transformed with respect to normal coordinates by $(\partial\mu_u/\partial Q_i) = \sum_j (\partial\mu_u/\partial X_j)L_{ij}$, where Q_i is the i^{th} normal coordinate, X_j is the j^{th} Cartesian displacement coordinate, and L_{ij} is the transformation matrix between the Cartesian displacement coordinates and the normal coordinates. The infrared intensities were then calculated by $[(N\pi)/(3c^2)]\,[(\partial\mu_x/\partial Q_i)^2 + (\partial\mu_y/\partial Q_i)^2 + (\partial\mu_z/\partial Q_i)^2]$. A comparison of experimental and simulated infrared spectra of cyclobutyldichlorosilane is shown in Fig. 2**.** Infrared spectrum of the gas and the predicted infrared spectra of the pure Eq-g, Eq-t, Ax-t and Ax-g conformers, and the mixture of the four conformers with relative concentrations calculated for the equilibrium mixture at 25ºC by using the experimentally determined enthalpy difference are shown in Fig. 2 (A-F). The predicted spectrum is in good agreement with the experimental spectrum which shows the utility of the scaled predicted frequencies and predicted intensities for supporting the vibrational assignment.

Additional support for the vibrational assignments was obtained from the simulated Raman spectra. The evaluation of Raman activity by using the analytical gradient methods has been developed[21–24] and the activity S_j can be expressed as: $S_j = g_j(45\alpha_j^2 + 7\beta_j^2)$, where g_j is the degeneracy of the vibrational mode j, α_j is the derivative of the isotropic polarizability, and β_j is the anisotropic polarizability. To obtain the Raman scattering cross sections, the polarizabilities are incorporated into S_j by multiplying S_j with $(1-\rho_j)/(1+\rho_j)$ where ρ_j is the depolarization ratio of the j^{th} normal mode. The Raman scattering cross sections and calculated wavenumbers obtained from the Gaussian 03 program were used together with a Lorentzian function to obtain the simulated Raman spectra. The Raman spectra of the liquid and the predicted Raman spectra for the four forms and the mixture of the four conformers with relative concentrations are obtained by

using the predicted enthalpy differences and is shown in Fig. 3(A-F). The spectrum of the mixture should be compared to that of the Raman spectrum of the liquid at room temperature. The predicted spectrum is in reasonable agreement0 with the experimental spectrum which shows the utility of the predicted Raman spectra for the supporting vibrational assignments.

4. Results

4.1. Vibrational assignment

Vibrational assignments for all four possible conformers of cyclobutyldichlorosilane are not reported in the literature. In order to determine the enthalpy difference between the stable conformers, it is essential to have a confident assignment for all of the fundamentals of the stable forms and identify vibrations which cannot be assigned to these conformers. The vibrations of the CH_2 group are expected to be very similar to those found in the usual four membered rings with just carbon atoms so their assignments are not discussed unless it is important. Therefore, the assignments of the six fundamentals of the ring will be provided along with fundamental modes involving the CSi, SiCl and SiH modes.

A strong band observed at 2204 cm^{-1} in the infrared spectra of the sample in gaseous form and the Raman spectra of the sample in liquid form are assigned for the SiH stretch fundamental mode of the Eq-g, Eq-t, Ax-t and Ax-g conformers of cyclobutyldichlorosilane. The Eq-g form has C_1 group symmetry and all thirty nine vibrational modes are in one single block (Table 1). A band observed at 1000 cm^{-1} in the infrared spectra of the sample in gaseous form is assigned for the ring breathing (ν_{21}) mode. In the same spectra bands observed at 937, 912 and 876 cm^{-1} are assigned for four ring deformation (ν_{22}, ν_{23}, ν_{24} and ν_{25}) fundamental modes. The SiH out-of-plane (ν_{26}) bend and SiH in-plane bend (ν_{27}) fundamental modes are assigned for strong bands observed at 800 and 791 cm^{-1} respectively in the infrared spectra of the sample in gaseous form. The band observed at 756 cm^{-1} in the infrared spectra of gaseous form of sample is assigned for the β-CH_2 rock (ν_{28}) fundamental mode. Interestingly, the γ-CH_2 rock (ν_{29}) fundamental mode was not observed and thus not assigned in the infrared spectra of the sample in gaseous form but bands observed at 701 and 703 cm^{-1} in the Raman spectra of the liquid sample and sample dissolved in liquid krypton are assigned for this mode. A strong band observed at 576 cm^{-1} in the infrared spectra of sample in gaseous form is assigned for the $SiCl_2$ antisymmetric stretch (ν_{30}) fundamental mode. The Si-C stretch (ν_{31}) fundamental mode was assigned for a band observed at 552 cm^{-1} in

the infrared spectra of sample in gaseous form. The same mode is assigned for bands observed at 548 and 560 cm^{-1} in the Raman spectra of liquid sample and sample dissolved in liquid krypton. Bands observed at 478, 479 and 482 cm^{-1} in the infrared spectra of sample in the gaseous form, Raman spectra of sample in liquid form and sample dissolved in liquid krypton respectively are assigned to the $SiCl_2$ symmetric stretch (ν_{32}) fundamental mode. Two $SiHCl_2$ ring bends (ν_{33} and ν_{34}) are assigned for bands observed at 385 and 284 cm^{-1} in the Raman spectra of the liquid sample. Additionally bands observed at 204 and 181 cm^{-1} in the Raman spectra of the liquid sample are assigned for the ring puckering (ν_{35}) and the $SiCl_2$ deformation (ν_{36}) modes respectively.

The Ax-t conformer of cyclobutyldichlorosilane has C_s group symmetry and its vibrational modes are divided into A′ and A″ blocks (Table 2) respectively. Twenty three vibrations are in the A′ block and sixteen vibrations are in the A″ block. The ring breathing, ring deformation 1, ring deformation 2 and ring puckering are symmetric with respect to the plane and hence all these modes are in the A′ block. A small intensity band observed at 1009 cm^{-1} in the infrared spectra of gaseous sample is assigned for the ring breathing (ν_{13}) fundamental mode. Similarly ring deformation 1 (ν_{14}) and ring deformation 2 (ν_{15}) fundamental modes are assigned to bands observed at 912 and 876 cm^{-1} respectively in the infrared spectra of sample in gaseous form. The SiH in-plane bend (ν_{16}) fundamental mode is assigned to bands which were observed at 780 and 777 cm^{-1} in the Raman spectra of liquid sample and in the sample dissolved in liquid krypton. Similarly the band observed at 680 cm^{-1} in the infrared spectra of gaseous sample is assigned for the Si-C stretch (ν_{17}) fundamental mode. The γ-CH_2 rock (ν_{18}) fundamental mode was assigned to Raman bands observed at 639 and 641 cm^{-1} in the Raman spectra of liquid sample and the sample dissolved in liquid krypton respectively. A medium intensity peak observed at 519 cm^{-1} in the infrared spectra of gaseous sample is assigned for the $SiCl_2$ symmetric stretch (ν_{19}) fundamental mode. Small intensity bands observed at 284, 220 and 161 cm^{-1} in the Raman spectra of the liquid sample are assigned for the $SiCl_2$ deformation (ν_{20}), ring puckering (ν_{21}) and $SiCl_2$ wag (ν_{22}) fundamental modes respectively.

In the A" block the ring deformation 1 (ν_{32}) fundamental mode is assigned for a band observed at 937 cm^{-1} in the infrared spectra of gaseous sample. Bands observed at 947 and 944 cm^{-1} in the Raman spectra of the sample in liquid form and the sample dissolved in liquid krypton respectively are assigned for the same mode. The ring deformation 2 (ν_{33}) fundamental mode is

assigned to very small intensity peaks observed at 911 and 912 cm^{-1} in the Raman spectra of the liquid and sample dissolved in liquid krypton respectively. The SiH out-of-plane bend (ν_{34}) mode is assigned to a band observed at 800 cm^{-1} in the infrared spectra of sample in gaseous form. In the same spectra a strong intensity band observed at 576 cm^{-1} is assigned for the $SiCl_2$ antisymmetric stretch (ν_{36}) fundamental mode which is predicted at 578 cm^{-1}. The $SiHCl_2$ ring bend (ν_{37}) fundamental mode is assigned for a band observed at 284 cm^{-1} in the Raman spectra of liquid sample.

Similar to Eq-g conformer the Ax-g conformer of cyclobutyldichlorosilane has C_1 group symmetry and all thirty nine vibrational modes are in one single block (Table 3). The β-CH_2 rock (ν_{19}) and β-CH_2 twist (ν_{20}) fundamental modes are assigned for bands observed at 1031 and 1021 cm^{-1} in the infrared spectra of the gaseous sample. In the same spectra a small intensity peak observed at 1009 cm^{-1} is assigned for the ring breathing (ν_{21}) fundamental mode. The ring deformation fundamental 1 (ν_{22}) mode is assigned for small intensity band observed at 947 and 950 cm^{-1} in the Raman spectra of sample in liquid form and the sample dissolved in liquid krypton respectively. Similarly bands observed at 937 and 912 cm^{-1} in the infrared spectra of gaseous sample are assigned for the ring deformation 1 (ν_{23}) and ring deformation 2 (ν_{24}) fundamental modes. The next ring deformation 2 (ν_{25}) fundamental mode are assigned to the bands observed at 857 and 860 cm^{-1} in the Raman spectra of the liquid form and sample dissolved in liquid krypton. The SiH out-of-plane (ν_{26}) and SiH in-plane bend (ν_{27}) modes are assigned for strong intensity bands observed at 791 and 767 cm^{-1} in the infrared spectra of sample in gaseous form. The β-CH_2 rock (ν_{28}) mode is assigned to the band observed at 767 cm^{-1} in the infrared spectra of sample in gaseous form and Raman spectra of liquid sample dissolved in krypton. The Si-C stretch (ν_{30}) fundamental mode is assigned for a band observed at 629 cm^{-1} in the infrared spectra of sample in gaseous form. The same fundamental mode is assigned at 630 and 636 cm^{-1} in the Raman spectra of sample in liquid form and sample dissolved in liquid krypton respectively. The $SiCl_2$ antisymmetric stretch (ν_{31}) and $SiCl_2$ symmetric stretch (ν_{32}) modes are assigned for a strong band observed at 568 and 492 cm^{-1} in the infrared spectra of sample in gaseous form. In the same spectra a band observed at 382 cm^{-1} is assigned for the $SiHCl_2$ ring bend (ν_{33}) fundamental mode. Bands observed at 291, 189 and 167 cm^{-1} in the Raman spectra of the liquid sample are assigned for the $SiHCl_2$ ring bend (ν_{34}), $SiCl_2$ deformation (ν_{35}) and ring puckering (ν_{36}) modes respectively.

The Eq-t conformer of cyclobutyldichlorosilane has C_s group symmetry and its vibrational modes are divided into A′ and A″ blocks (Table 4). Similar to Ax-t conformer, for the Eq-t form twenty three vibrations are in A′ block and sixteen vibrations are in A″ block. In the A′ block the ring breathing (ν_{13}) fundamental mode is assigned for a weak intensity band observed at 1000 cm^{-1} in the infrared spectra of sample in gaseous form. The ring deformation 1 (ν_{14}) and ring deformation 2 (ν_{15}) fundamental modes which are symmetric with respect to the plane are assigned for bands observed at 912 and 876 cm^{-1} respectively in the infrared spectra of the gaseous sample. In the same spectra a strong intensity band which is predicted at 787 cm^{-1} and is observed at 791 cm^{-1} is assigned for the SiH in-plane bend (ν_{16}) mode. The γ-CH_2 rock mode (ν_{17}) is assigned for a band observed at 717 cm^{-1} in the infrared spectra of the sample in gaseous form and also observed at the same frequency in the Raman spectra of the liquid sample. The same fundamental mode is assigned for a band observed at 719 cm^{-1} in the Raman spectra of the sample dissolved in liquid krypton. A medium intensity band observed at 568 cm^{-1} in the infrared spectra of the sample is assigned for the Si-C stretch (ν_{18}) mode. Similarly the $SiCl_2$ symmetric stretch (ν_{19}) mode is assigned for a band observed at 519 cm^{-1} in the infrared spectra of the gaseous sample. Bands observed at 284 and 159 cm^{-1} in the Raman spectra of the liquid sample are assigned for the ring puckering (ν_{20}) and $SiCl_2$ deformation (ν_{21}) modes.

In the A″ block of the Eq-t conformer ring deformation 1 (ν_{32}) and ring deformation 2 (ν_{33}) modes are predicted at 936 and 933 cm^{-1} respectively. Prediction of these fundamental modes are so close to each other that, instead of two different bands, a single band should be expected. Weak intensity bands are observed at 937, 934 and 935 cm^{-1} in the infrared spectra of the sample in the gaseous form, the Raman spectra of sample in liquid form and Raman spectra of krypton solution respectively and are assigned to the ring deformation 1 (ν_{32}) and ring deformation 2 (ν_{33}) fundamental modes. The SiH out-of-plane bend (ν_{34}) fundamental mode is assigned for a band observed at 800 cm^{-1} in the infrared spectra of the sample in the gaseous form. In the same spectra, a band is observed at 771 cm^{-1} and assigned to the β-CH_2 rock (ν_{35}) mode. The $SiCl_2$ antisymmetric stretch (ν_{36}) mode is assigned to a band observed at 576 cm^{-1} in the infrared spectra of the sample in the gaseous form. A small intensity band observed at 284 cm^{-1} in the Raman spectra of the liquid sample is assigned to the $SiHCl_2$ ring bend (ν_{37}) mode.

Notable mixing of the different vibrational modes of cyclobutyldichlorosilane with the assigned vibrational mode are observed in ν_{15}, ν_{18}, ν_{21}, ν_{29}, ν_{31}, ν_{34} and ν_{37} vibrational modes of Eq-g conformer. In these vibrational modes, the mixing of vibrational modes with one another is so significant that the contribution of the assigned fundamental mode became considerably low. Same patterns are observed for the ν_{10}, ν_{11}, ν_{12}, , ν_{20}, ν_{21}, $\nu_{23,}$ ν_{29} and ν_{30} vibrational modes of the Ax-t conformer, for ν_{10}, ν_{12}, ν_{15}, ν_{17}, ν_{18}, ν_{20}, ν_{21}, ν_{30}, ν_{31} and the ν_{33} vibrational modes of the Eq-t conformer and also for the ν_{14}, ν_{16}, ν_{17}, ν_{18}, ν_{19}, ν_{20}, ν_{33}, ν_{34} and ν_{37} vibrational modes of the Ax-g conformer of cyclobutyldichlorosilane. The mixing of different vibrational modes are responsible for large error between predicted and experimental observed frequencies. With these assignments, the remaining vibrational modes are easily assigned so the assignments for the fundamentals for this molecule are confidently made.

4.2. Conformational stability

The enthalpy difference values between the four conformers were experimentally measured and used to determine the stability. The enthalpy values were measured using variable temperature Raman spectra of the sample dissolved in liquid krypton (Fig. 4) at three different temperatures between -143 and -123°C. Relatively small interactions are expected to occur between xenon and the sample but the sample can associate with itself through van der Waals interactions. However, due to the very small concentration of sample (~10^{-4} molar), self-association is greatly reduced. Therefore, only small wavenumber shifts are anticipated between krypton and the sample when krypton passes from the gas phase to the liquid. A significant advantage of this study is that the conformer bands are better resolved in comparison with those in the infrared spectrum of the gas (Fig. 5A-B).

Using the vibrational assignments for the four conformers (Tables 1-4), specific bands from each conformer were chosen to measure the enthalpy differences. These bands are carefully chosen to minimize the effect of combination and overtone bands in the enthalpy determination. Therefore it is desirable to have the lowest frequency pairs possible for the determination. The bands should also be sufficiently resolved so reproducible intensities can be obtained. Therefore all bands used in determining the enthalpy difference were below 1000 cm^{-1}.

The intensities of the individual bands were measured as a function of temperature and their ratios were determined. By application of the van't Hoff equation $-\ln K = \Delta H/(RT) - \Delta S/R$,

the enthalpy differences were determined from a plot of –lnK versus 1/T, where ΔH/R is the slope of the line and K is substituted with the appropriate intensity ratios, i.e. I_{conf-1} / I_{conf-2}, etc. It was assumed that ΔS is not a function of temperature in the range studied.

Due to significant mixing, only a limited number of band pairs were used to determine the enthalpy differences between each conformer. The following bands were used to determine the enthalpy difference values: two bands at 560 cm^{-1} and 703 cm^{-1} for the Eq-g conformer, one band at 944 cm^{-1} for the Ax-t conformer, one band at 636 cm^{-1} for the Ax-g conformer, and two bands at 719 cm^{-1} and 935 cm^{-1} for the Eq-t conformer. The intensities for each band and temperature were determined using Fityk software package [25] and utilizing the Voight fit function. The advantage to using the Voight fit function is that it contains both Gaussian and Lorenztian profiles which maximizes the accuracy of the fit. The ratio of intensities for each conformer were placed in Table 6. Each band pair ratio and their respective enthalpy differences were used to obtain an average enthalpy difference. The statistical average values with standard deviation of one sigma were obtained by treating all the data as a single set and are given in Table 6.

The variable temperature Raman spectra (-143 to -123 ^{0}C) of the krypton solution determined the stability of the four possible conformers of cyclobutyldichlorosilane. The Eq-g conformer was determined to be the most stable followed by Ax-t, Eq-t, and Ax-g. The sample is estimated to contain 47% of the Eq-g conformer at room temperature. The other conformers are estimated to be 16 ± 1 % for Ax-t, 13 ± 2 % for Eq-t, and 24 ± 4 % for Ax-g. With the exception of the Eq-t conformer, the predictions are in good agreement with the experimental work where Eq-g is the most stable conformer followed by Ax-t and Ax-g. The energy difference between the Eq-g and Eq-t forms are somewhat unclear when comparing the predictions to the experimental work. This discrepancy will be elaborated on in the discussion section of this work.

5. Discussion

Average and percent errors were calculated between predicted and observed frequencies for all four conformers of the cyclobutyldichlorosilane. For the Eq-g conformer the average error was determined to be 5.51 cm^{-1} which represents a percent error of 0.24%. Similarly for Ax-t, Ax-g and Eq-t conformers of cyclobutyldichlorosilane the average error was calculated to be 5.5, 6.28 and 6.6 cm^{-1} which represents a percent error of 0.30, 0.29 and 0.32% respectively. Both the

average and percent errors are reasonable and show that predicted frequencies are meaningful with respect to the vibrational assignments.

Interesting trends are observed for the C-Si stretch, ring breathing and $SiCl_2$ symmetric stretch modes of all conformers of cyclobutyldichlorosilane in the infrared spectra of the gas. The C-Si stretch modes are observed at 568 and 552 cm^{-1} for the Eq-t and Eq-g conformers respectively. The same mode is observed at 680 cm^{-1} for the Ax-t and at 629 cm^{-1} for the Ax-g forms. So the C-Si stretch modes are observed at lower frequencies for the gauche conformer compared to the trans conformer of both Eq and Ax forms. Additionally, frequencies observed for the Eq conformer for the C-Si stretch mode are lower than the frequencies observed for the Ax form. The same pattern is observed for cyclobutylsilane where the C-Si stretch mode was assigned at lower frequency for the Eq conformer compared to the Ax form[11]. Similarly, the ring breathing and $SiCl_2$ symmetric stretch modes for cyclobutyldichlorosilane are predicted and assigned at lower frequencies for the Eq conformer compared to the Ax form. However for cyclobutylsilane the ring breathing mode was assigned at higher frequency for the Eq conformer compared to the Ax form[11]. Overall when two chlorine atoms are substituted on the cyclobutyl moiety, the pattern for the C-Si stretch modes remains the same but the trend does not follow for the ring breathing modes.

The ab initio calculations were carried out for this molecule and the energy differences (Table 5) for the four possible forms were obtained with the Eq-t form as the most stable conformer followed by the Eq-g, Ax-t and Ax-g forms. The ab initio predicted energy difference from the MP2(full)/6-311G(d,p) calculations with 198 basis sets gave the Eq-t conformer as the more stable form by 57 cm^{-1} (0.68 kJ/mol) than the Eq-g form. The B3LYP method with all the basis sets used in this study consistently predicts Eq-t as the more stable conformer followed by Eq-g, Ax-t and Ax-g forms, respectively. From the band intensities of the Eq-t and Eq-g $SiCl_2$ symmetric stretch fundamentals assigned at 518 and 482 cm^{-1}, respectively, an initial ΔH can be determined with a value of 271 cm^{-1}. The accuracy of this value is likely to be very poor as there are underlying fundamentals from the Ax-t and Ax-g fundamentals in near coincidence with these two bands but this can give an idea of which conformer is more stable and it gives a value to compare the predicted energy differences.

It is interesting to note that proceeding to a higher basis set (i.e. MP2(full)/6-311+G(2d,2p)) it predicts the Eq-g form to be more stable than the Eq-t conformer by 82 cm^{-1}. This is an interesting

phenomenon where the addition of more functions into the ab initio basis sets actually causes more inconsistent results. The same basis set using the B3LYP method instead gave the Eq-t form as the most stable conformer from the four possible ones. The ab initio predicted MP2(full) values predict the Eq-g conformer as being the more stable form. Thus the B3LYP method gives more consistent results for conformational stability predictions in this study compared to the MP2(full) calculation which was not able to predict a specific conformer as the more stable form. The experimentally determined enthalpy differences obtained in this study should be comparable to the ab initio predicted energy values and also can be compared with other enthalpy differences obtained for other molecules of the form c-$C_4H_7SiHX_2$. The B3LYP predictions appear to correspond much better with the experimental result and so are thought to be more reliable for the determination of the energy differences.

The experimental results show that Eq-g is the most stable conformer followed by Ax-t, Eq-t and then Ax-g. It is interesting to note that the experimentally determined energy differences are in some disagreement with the ab initio predictions. The predictions also showed conflicting results where either the Eq-g or Eq-t conformer could be the most stable. The experimental results however indicate that Ax-t is more stable than Eq-t. Upon consideration of the error for each enthalpy difference, it is possible that Eq-t could be more stable than the Ax-t form. Further studies would be needed to confirm the exact difference. In previous studies, the equatorial conformer was determined to be the more stable conformer for cyclobutylsilane [11] and cyclobutyltrifluorosilane [26]. Therefore the stability of cyclobutyldichlorosilane is in good agreement with previous studies of similar molecules. It would be of interest to study other cyclobutyldihalosilanes and compare them to this study.

Additionally it would also be of interest to obtain the complete adjusted r_0 structural parameters for the stable conformers of cyclobutyldichlorosilane. To do so, predicted rotational constants need to be fitted from the microwave spectra using suitable predicted structures (Table 7). We [27] have shown that ab initio MP2(full)/6-311+G(d,p) calculations predict the carbon-hydrogen r_0 structural parameters for more than fifty hydrocarbons to at least 0.002 Å compared to the experimentally determined values [28] from isolated CH stretching frequencies which agree with previously determined values from earlier microwave studies. Therefore, all of the carbon-hydrogen parameters can be taken from the MP2(full)/6-311+G(d,p) predicted values for the conformers of cyclobutyldichlorosilane. The silane-hydrogen r_0 structural parameter value was experimentally

determined [28] for the Eq-t conformer to be 1.477(2) Å from isolated SiH stretching frequency listed in Table 2. This leaves 9 independent structural parameters to be determined for completed adjusted r_0 structural parameters. Therefore a minimum of 9 rotational constants would be desirable to obtain such an experimental structure. Additionally, we have also shown that the differences in predicted distances and angles from the ab initio calculations for different conformers of the same molecule can usually be used as one parameter with the ab initio predicted differences except for some dihedral angles. This would mean that each additional conformer would only increase the minimum number of rotational constants by three. Such a microwave study would be desirable as there are few cyclobutylsilane structures determined, but the study of the microwave spectra of cyclobutyldichlorosilane will be a challenging investigation with a high degree of difficulty. This difficulty is due to the Cl atoms on the Si substituent where each chlorine nucleus has a spin quantum number I = 3/2 and, therefore, a nuclear quadrupole moment which interacts with the electric field gradient created by the electrons of the rotating molecule. Due to these reasons mentioned above the microwave study was not undertaken and the structural parameters were presented in the form of ab initio predictions only.

6. Conclusion

Vibrational assignments for all four conformers of cyclobutyldichlorosilane were made using the infrared spectra of the gas, Raman spectrum of the sample dissolved in liquid krypton and Raman spectra of the sample in the liquid state. The enthalpy difference and conformer stability were determined for the four conformers by using variable temperature Raman spectra dissolved in liquid krypton. Ab initio calculations with various basis sets were obtained for all four conformers of cyclobutyldichlorosilane by using both MP2(full) and B3LYP methods. We would like to continue our investigation into substituted cyclobutanes by investigating cyclobutyltrifluorosilane and cyclobutyldifluorosilane. It would be very interesting to observe what effect the fluorine atom has over the structure and conformer stability compared to the chlorine substitution in the current study.

Acknowledgement

JRD acknowledges the University of Missouri–Kansas City, for a Faculty Research Grant for partial financial support of this research. GAG gratefully acknowledges the partial financial support of this study by the Camille and Henry Dreyfus Foundation by grant no. SI-14-007 and the Undergraduate Research and Creative activities at the College of Charleston.

References

[1] R.C. Lord, I. Nakagawa, J. Chem. Phys. 39 (1963) 2951.

[2] T. Ueda, J. Chem. Phys. 49 (1968) 470.

[3] F.A. Miller, R.J. Capwell, R.C. Lord, D.G. Rea, Spectrochim. Acta 28A (1972) 603.

[4] W.G. Rothschild, J. Chem. Phys. 45 (1966) 1214.

[5] J.R. Durig, W.H. Green, J. Chem. Phys. 47 (1967) 673.

[6] C.S. Blackwell, L.A. Carreira, J.R. Durig, J.M. Karriker, R.C. Lord, J. Chem. Phys. 56 (1972) 1706.

[7] J. Durig, W. Green, N. Hammond, J. Phys. Chem. 70 (1966) 1989.

[8] H. Kim, W.D. Gwinn, J. Chem. Phys. 44 (1966) 865.

[9] J.R. Durig, A.C. Morrissey, J. Chem. Phys. 46 (1967) 4854.

[10] A. Wurstner-Rock, H.D. Rudolph, J. Mol. Struct. 97 (1983) 327.

[11] J.J. Klaassen, S.S. Panikar, G.A. Guirgis, H.W. Dukes, J.K. Wyatt, J.R. Durig, J. Mol. Struct. 1032 (2013) 254.

[12] J.R. Durig, I.D. Darkhalil, B.S. Deodhar, G.A. Guirgis, J.K. Wyatt, C.W. Reed, Asian J. Phys. 23 (2014) 861.

[13] B. Michielsen, J.J.J. Dom, B.J. van der Veken, S. Hesse, Z. Xue, M.A. Suhm, W.A. Herrebout, Phys. Chem. Chem. Phys. 12 (2010) 14034.

[14] W.A. Herrebout, N. Nagels, B.J. van der Veken, ChemPhysChem 10 (2009) 3054.

[15] D. Hauchecorne, R. Szostak, W.A. Herrebout, B.J. Van Der Veken, ChemPhysChem 10 (2009) 2105.

[16] M.J. Frisch, G.W. Trucks, H.B. Schlegel, G.E. Scuseria, M.A. Robb, J.R. Cheeseman, J.A. Montgomery, T. Vreven, K.N. Kudin, J.C. Burant, J.M. Millam, S.S. Iyengar, J. Tomasi, V. Barone, B. Mennucci, M. Cossi, G. Scalmani, N. Rega, G.A. Petersson, H. Nakatsuji, M. Hada, M. Ehara, K. Toyota, R. Fukuda, J. Hasegawa, M. Ishida, T. Nakajima, Y. Honda, O. Kitao, H. Nakai, M. Klene, X. Li, J.E. Knox, H.P. Hratchian, J.B. Cross, V. Bakken, C. Adamo, J. Jaramillo, R. Gomperts, R.E. Stratmann, O. Yazyev, A.J. Austin, R. Cammi, C. Pomelli, J.W. Ochterski, P.Y. Ayala, K. Morokuma, G.A. Voth, P. Salvador, J.J. Dannenberg, V.G. Zakrzewski, S. Dapprich, A.D. Daniels, M.C. Strain, O. Farkas, D.K. Malick, A.D. Rabuck, K. Raghavachari, J.B. Foresman, J. V Ortiz, Q. Cui, A.G. Baboul, S. Clifford, J. Cioslowski, B.B. Stefanov, G. Liu, A. Liashenko, P. Piskorz, I. Komaromi, R.L. Martin, D.J. Fox, T. Keith, A.M.A. Laham, C.Y. Peng, A. Nanayakkara, M. Challacombe, P.M.W. Gill, B. Johnson, W. Chen, M.W. Wong, C. Gonzalez, J.A. Pople, Gaussian 03, Revision C.02, Gaussian, Inc., Wallingford CT, 2004.

[17] P. Pulay, Mol. Phys. 17 (1969) 197.

[18] C. Møller, M.S. Plesset, Phys. Rev. 46 (1934) 618.

[19] G.A. Guirgis, X. Zhu, Z. Yu, J.R. Durig, J. Phys. Chem. A 104 (2000) 4383.

[20] P. Larkin, Infrared and Raman Spectroscopy Principles and Spectral Interpretation, 1st ed., Elsevier, Amsterdam, 2011.

[21] M.J. Frisch, Y. Yamaguchi, J.F. Gaw, H.F. Schaefer, J.S. Binkley, J. Chem. Phys. 84 (1986) 531.

[22] R.D. Amos, Chem. Phys. Lett. 124 (1986) 376.

[23] P.L. Polavarapu, J. Phys. Chem. 94 (1990) 8106.

[24] G.W. Chantry, A. Anderson, The Raman Effect, 1st ed., Maarcel Dekker Inc., New York, 1971.

[25] M. Wojdyr, J. Appl. Crystallogr. 43 (2010) 1126.

[26] J.R. Durig, M. Dakkouri, T.K. Gounev, P. Zhen, J. Mol. Struct. 516 (2000) 161.

[27] J.R. Durig, W.N. Kar, C. Zheng, S. Shen, Struct. Chem. 15 (2004) 149.

[28] D.C. McKean, J. Mol. Struct. 113 (1984) 251.

Figure Captions

Fig. 1. Conformers of cyclobutyldichlorosilane.

Fig. 2. Comparison of experimental and calculated infrared spectra of cyclobutyldichlorosilane: (A) observed spectrum of gas; (B) simulated spectrum of a mixture of the four stable conformers of cyclobutyldichlorosilane at 25°C; (C) simulated spectrum of Ax-g conformer; (D) simulated spectrum of Ax-t conformer; (E) simulated spectrum of Eq-t conformer; (F) simulated spectrum of conformer Eq-g.

Fig. 3. Comparison of experimental and calculated Raman spectra of cyclobutyldichlorosilane (A) observed spectrum in liquid (B) simulated spectrum of a mixture of the four stable conformers of cyclobutyldichlorosilane at 25°C; (C) simulated spectrum of Ax-g conformer; (D) simulated spectrum of Ax-t conformer; (E) simulated spectrum of Eq-t conformer; (F) simulated spectrum of conformer Eq-g.

Fig. 4. Raman spectra (1550 to 350 cm-1) of temperature dependent (-143 to -123°C) band intensities for the four conformers of cyclobutyldichlorosilane dissolved in liquid krypton.

Fig. 5. Comparison spectra of cyclobutyldichlorosilane: (A) infrared gas in transmittance; (B) Raman spectra in krypton solution at -143°C in absorbance. Labelled bands were used for enthalpy determinations.

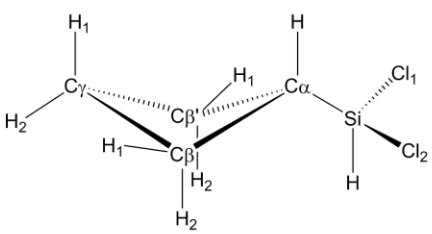

Ax-t

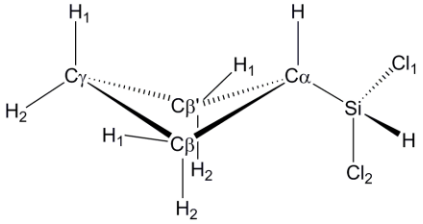

Ax-g

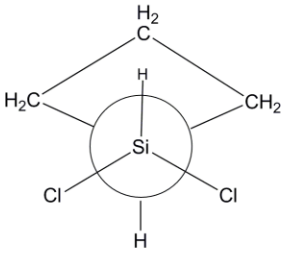

Eq-t

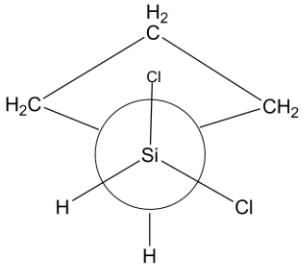

Eq-g

Fig. 1

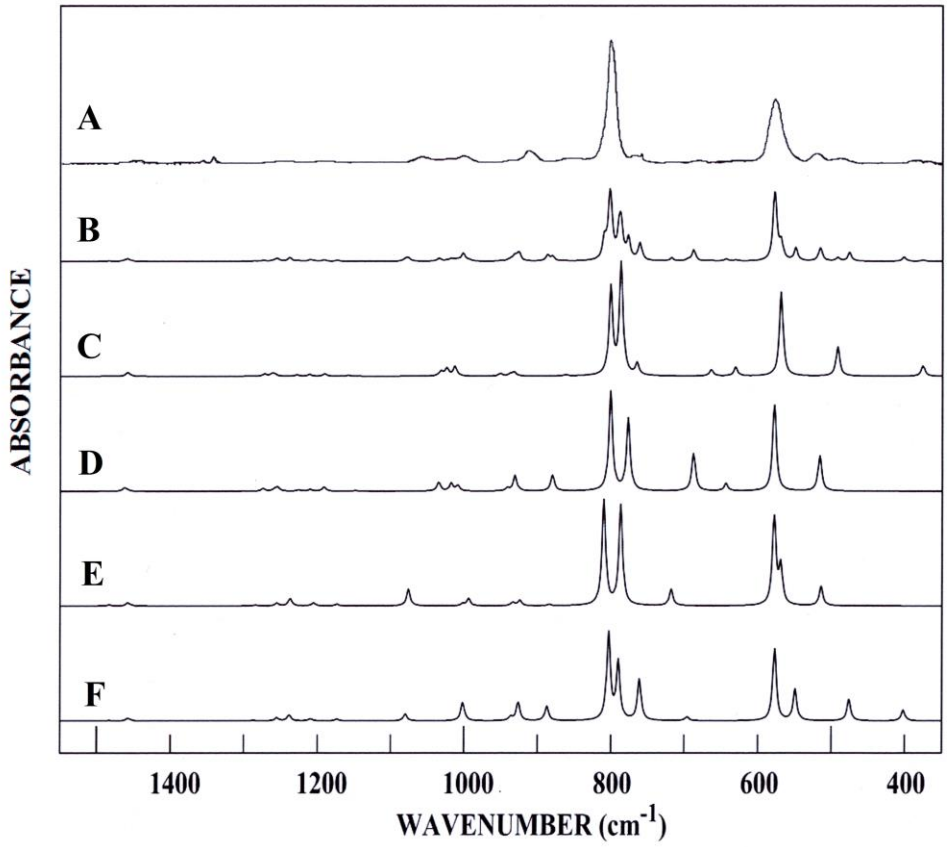

Fig. 2

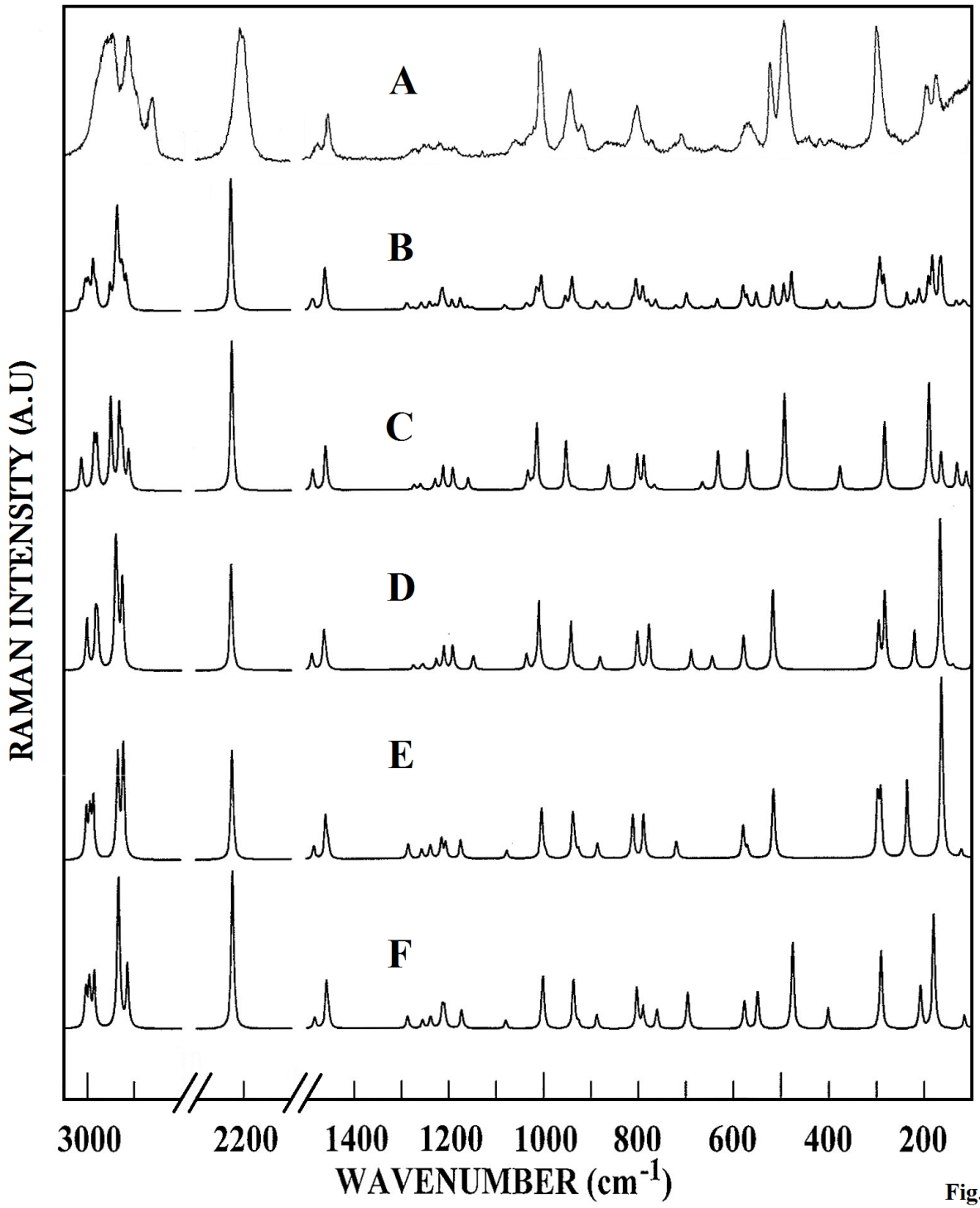

Fig. 3

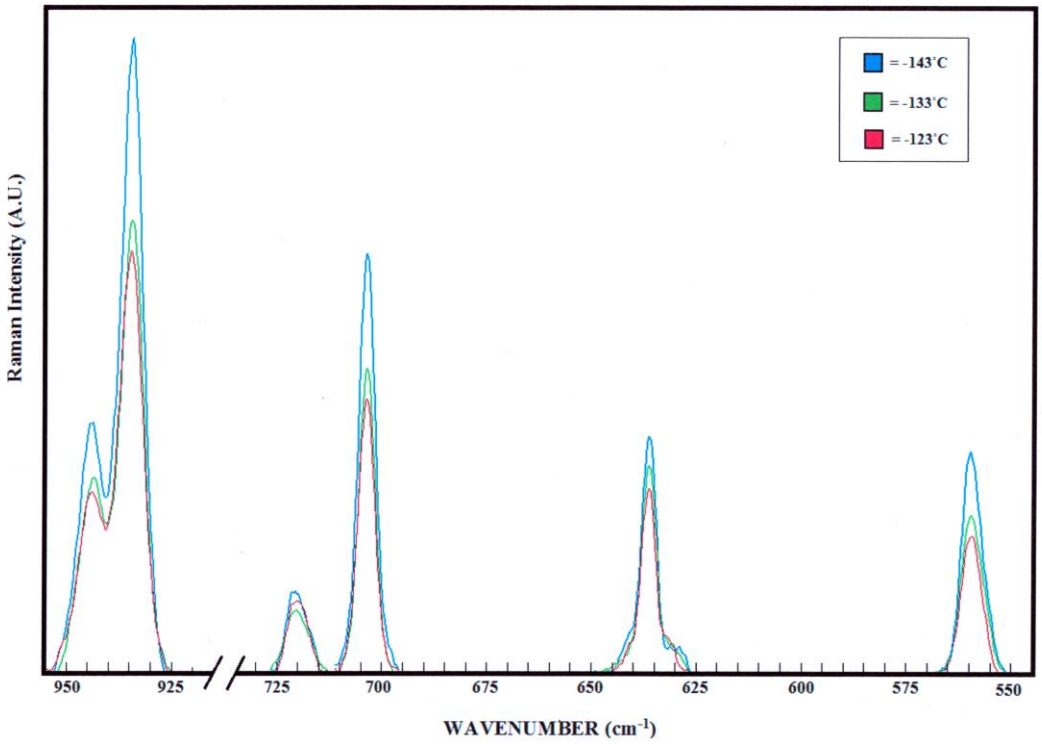

Fig. 4

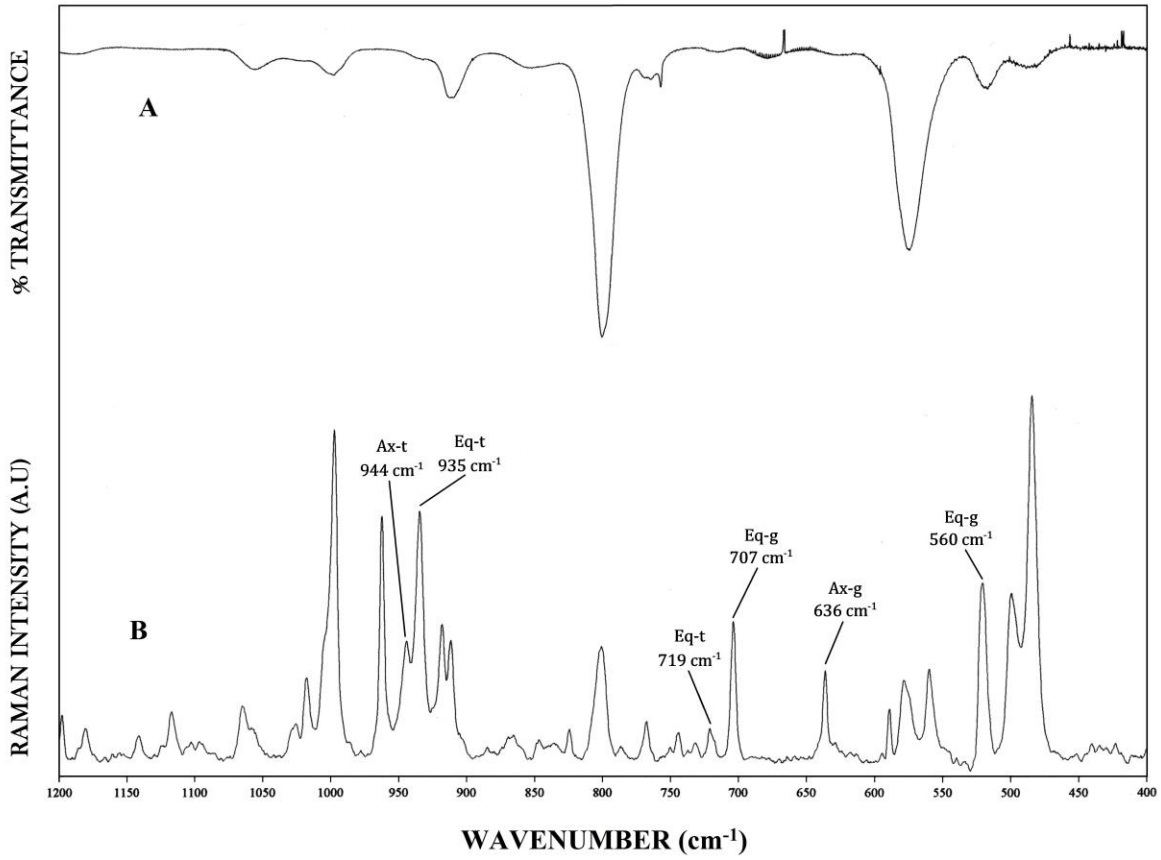

Fig. 5

Table 1. Observed and calculated[a] frequencies (cm^{-1}) for Eq-g cyclobutyldichlorosilane.

	Vib. No.	Approximate Descriptions	ab initio	fixed scaled[b]	IR int.	Raman act.	dp ratio	IR	Raman		P.E.D.[c]	Band Contours[d]		
								Gas	Liquid	Krypton		A	B	C
	ν_1	β-CH_2 antisymmetric stretch	3201	3003	33.8	53.0	0.68	2996	2994	2986	$59S_1$, $36S_3$	-	84	16
	ν_2	β-CH_2 antisymmetric stretch	3193	2995	17.0	64.0	0.75	2996	2989	2985	$93S_2$	5	3	92
	ν_3	γ-CH_2 antisymmetric stretch	3182	2985	8.0	75.5	0.45	2984	~2969	2970	$58S_3$, $36S_1$	95	3	3
	ν_4	β-CH_2 symmetric stretch	3128	2934	9.4	147.8	0.04	2934	2948	2947	$75S_4$, $12S_6$	36	2	62
	ν_5	β-CH_2 symmetric stretch	3126	2932	35.0	45.9	0.12	2934	2948	2947	$62S_5$, $36S_6$	66	8	26
	ν_6	γ-CH_2 symmetric stretch	3125	2931	26.7	45.0	0.66	2934	2948	2936	$50S_6$, $28S_5$, $21S_4$	30	31	39
	ν_7	CH stretch	3107	2914	11.6	84.0	0.31	2905	~2900	2902	$98S_7$	14	53	33
	ν_8	SiH stretch	2343	2223	136.5	138.5	0.16	2204	2204	2208	$100S_8$	9	2	89
	ν_9	β-CH_2 deformation	1575	1483	0.7	5.5	0.70	-	-	-	$68S_9$, $30S_{10}$	36	51	13
	ν_{10}	γ-CH_2 deformation	1549	1458	3.9	21.4	0.72	1461	~1465	-	$69S_{10}$, $32S_9$	15	70	15
	ν_{11}	β-CH_2 deformation	1544	1454	1.2	5.2	0.75	1448	1443	-	$100S_{11}$	7	26	67
	ν_{12}	β-CH_2 wag	1354	1287	0.9	4.9	0.70	-	-	-	$51S_{12}$, $26S_{15}$, $15S_{17}$	6	80	15
	ν_{13}	γ-CH_2 wag	1322	1255	4.9	3.2	0.75	1248	~1258	-	$71S_{13}$	14	20	67
	ν_{14}	β-CH_2 wag	1306	1239	1.9	1.2	0.70	1234	1243	~1236	$53S_{14}$, $13S_{20}$, $13S_{16}$	45	53	2
	ν_{15}	CH in-plane bend	1302	1238	7.5	3.4	0.75	1234	1243	1236	$28S_{15}$, $32S_{12}$, $17S_{17}$	26	41	33
	ν_{16}	CH out-of-plane bend	1279	1214	0.3	7.9	0.75	1202	1211	~1216	$47S_{16}$, $24S_{18}$, $10S_{13}$	32	12	56
	ν_{17}	β-CH_2 twist	1270	1209	3.2	7.3	0.73	1202	1211	1216	$44S_{17}$, $19S_{29}$, $12S_{15}$,$12S_{21}$	68	17	15

	ν_{18}	γ-CH_2 twist	1235	1173	3.1	6.7	0.75	-	1178	1081	$25S_{18}$, $33S_{14}$, $22S_{20}$	22	18	60
	ν_{19}	β-CH_2 rock	1132	1080	10.7	2.6	0.18	1056	1054	~1052	$30S_{19}$, $28S_{21}$	97	-	3
	ν_{20}	β-CH_2 twist	1055	1002	19.3	6.7	0.24	1000	~998	~997	$22S_{20}$, $19S_{19}$, $17S_{22}$, $11S_{23}$	58	2	40
	ν_{21}	Ring breathing	1049	1001	10.8	9.5	0.16	1000	~998	997	$10S_{21}$, $37S_{19}$, $11S_{15}$, $10S_{20}$	3	94	3
	ν_{22}	Ring deformation 2	986	937	1.3	7.0	0.75	937	934	939	$40S_{22}$, $29S_{23}$, $11S_{13}$	-	14	86
	ν_{23}	Ring deformation 1	975	936	4.7	6.9	0.75	937	934	939	$44S_{23}$, $20S_{20}$, $14S_{16}$	56	7	37
	ν_{24}	Ring deformation 1	961	926	29.2	1.4	0.11	~912	911	916	$55S_{24}$, $11S_{12}$, $10S_{31}$	67	32	1
	ν_{25}	Ring deformation 2	917	887	23.0	3.6	0.14	876	-	~876	$41S_{25}$, $21S_{29}$, $10S_{21}$	20	72	9
	ν_{26}	SiH out-of-plane bend	846	803	139.4	9.2	0.75	800	~798	801	$95S_{26}$	22	78	-
	ν_{27}	SiH in-plane bend	831	790	91.7	4.8	0.75	~791	785	~787	$43S_{27}$, $30S_{28}$	82	12	7
	ν_{28}	β-CH_2 rock	800	761	65.4	4.0	0.72	756	764	767	$42S_{28}$, $27S_{27}$	99	1	-
	ν_{29}	γ-CH_2 rock	726	696	6.4	6.9	0.40	-	701	703	$28S_{29}$, $15S_{25}$, $12S_{27}$, $12S_{31}$	33	55	12
	ν_{30}	$SiCl_2$ antisymmetric stretch	605	577	115.1	4.1	0.75	~576	~577	580	$83S_{30}$	10	90	0
	ν_{31}	Si-C stretch	573	549	50.4	5.1	0.58	552	548	560	$16S_{31}$, $40S_{32}$, $20S_{25}$,	79	5	16
	ν_{32}	$SiCl_2$ symmetric stretch	497	476	34.5	9.8	0.02	~478	479	482	$46S_{32}$, $15S_{31}$, $10S_{25}$	2	21	77
	ν_{33}	$SiHCl_2$ Ring bending	412	402	17.4	1.9	0.61	-	385	392	$31S_{33}$, $31S_{37}$	35	52	13
	ν_{34}	$SiHCl_2$ Ring bending	297	291	2.4	4.4	0.35	-	~284	-	$33S_{34}$, $11S_{31}$, $11S_{38}$, $10S_{33}$, $10S_{32}$	55	1	44
	ν_{35}	Ring puckering	210	208	0.6	1.4	0.71	-	204	-	$48S_{35}$, $22S_{38}$, $12S_{36}$	-	75	25
	ν_{36}	$SiCl_2$ deformation	181	180	5.0	3.0	0.70	-	181	-	$77S_{36}$	35	20	45
	ν_{37}	$SiCl_2$ wag	116	115	3.1	0.8	0.63	-	-	-	$11S_{37}$,$42S_{33}$, $30S_{34}$,$10S_{39}$	50	-	50

	ν_{38}	$SiCl_2$ twist	97	96	1.8	1.0	0.73	-	-	-	$46S_{38}$, $33S_{37}$, $10S_{21}$	14	66	21
	ν_{39}	$SiCl_2$ rock	46	44	0.4	0.4	0.74	-	-	-	$82S_{39}$	33	4	63

[a] MP2(full)/6-31G(d) ab initio calculations, scaled frequencies, infrared intensities (km/mol), Raman activities ($Å^4$/amu), depolarization ratios and potential energy distributions (P.E.D.s)

[b] MP2(full)/6-31G(d) fixed scaled frequencies with factors of 0.88 for CH and SiH stretches and CH_2 deformations, 1.0 for heavy atom bends, and 0.90 for all other modes.

[c] Contributions less than 10% are omitted.

[d] A, B and C values in the last two columns are percentage infrared band contours.

Table 2. Observed and calculated[a] frequencies (cm^{-1}) for Ax-t cyclobutyldichlorosilane.

	Vib. No.	Approximate Descriptions	ab initio	fixed scaled[b]	IR int.	Raman act.	dp ratio	IR	Raman		P.E.D.[c]	Band Contours[d]	
								Gas	Liquid	Krypton		A	C
A′	ν_1	γ-CH_2 antisymmetric stretch	3198	3000	40.0	71.1	0.52	2996	2984	2987	$80S_1$, $19S_2$	78	22
	ν_2	β-CH_2 antisymmetric stretch	3173	2977	13.2	60.4	0.75	2974	2969	2968	$78S_2$, $18S_1$	1	99
	ν_3	γ-CH_2 symmetric stretch	3132	2938	10.4	167.9	0.06	2934	2948	2947	$84S_3$	54	46
	ν_4	CH stretch	3127	2933	24.4	48.6	0.23	2934	2948	2936	$76S_4$, $11S_3$,$10\ S_5$	41	59
	ν_5	β-CH_2 symmetric stretch	3117	2924	4.4	114.5	0.26	2924	2915	2923	$83S_5$, $15S_4$	96	4
	ν_6	SiH stretch	2345	2225	104.2	92.8	0.12	2204	2204	2208	$100S_6$	5	95
	ν_7	β-CH_2 deformation	1580	1488	0.5	8.0	0.64	-	-	-	$71S_7$, $28S_8$	52	48
	ν_8	γ-CH_2 deformation	1554	1463	4.6	16.8	0.75	1461	1465	-	$72S_8$, $29S_7$	1	99
	ν_9	β-CH_2 wag	1341	1274	3.8	1.8	0.57	-	1267	-	$49S_9$, $29S_{10}$, $14S_{11}$	72	28
	ν_{10}	CH in-plane bend	1316	1254	5.7	1.9	0.44	1248	1258	-	$15S_{10}$, $34S_9$, $26S_{11}$,$16S_{14}$	60	40
	ν_{11}	β-CH2 twist	1250	1191	6.2	8.9	0.74	1189	1192	1198	$33S_{11}$, $24S_{18}$, $18S_{12}$, $15S_{10}$	100	0
	ν_{12}	β-CH_2 rock	1087	1035	13.5	4.6	0.48	1031	-	1027	$32S_{12}$, $29S_{10}$	100	0
	ν_{13}	Ring breathing	1063	1009	8.4	20.4	0.12	1009	1006	1005	$83S_{13}$, $10S_{10}$	62	38
	ν_{14}	Ring deformation 1	966	931	24.4	0.1	0.34	~912	911	912	$70S_{14}$, $12S_9$	99	1
	ν_{15}	Ring deformation 2	909	880	24.7	3.3	0.56	876	-	876	$49S_{15}$, $22S_{18}$, $12S_{16}$	90	10
	ν_{16}	SiH in-plane bend	816	777	114.8	9.7	0.75	-	~780	777	$75S_{16}$	99	1
	ν_{17}	Si-C stretch	718	688	59.7	3.7	0.16	680	690	~703	$48S_{17}$, $14S_{15}$, $10S_{18}$	97	3
	ν_{18}	γ-CH_2 rock	668	644	11.9	2.3	0.40	-	~639	641	$30S_{15}$, $23S_{12}$, $21S_{18}$,$17S_{17}$	78	22
	ν_{19}	$SiCl_2$ symmetric stretch	540	516	56.3	10.1	0.09	519	~510	~522	$78S_{19}$	81	19

	ν_{20}	$SiCl_2$ deformation	289	282	0.2	4.1	0.14	-	~284	-	$10S_{20}$, $31S_{23}$,$17S_{21}$, $15S_{17}$, $13S_{19}$	99	1
	ν_{21}	Ring puckering	224	220	5.7	1.4	0.67	-	220	-	$34S_{21}$, $29S_{20}$, $27S_{22}$	0	100
	ν_{22}	$SiCl_2$ wag	165	165	6.1	3.4	0.74	-	161	-	$53S_{22}$, $40S_{20}$	81	19
	ν_{23}	$SiHCl_2$ Ring bending	141	139	5.0	0.1	0.46	-	-	-	$34S_{23}$, $47S_{20}$, $14S_{21}$	21	79
A''	ν_{24}	β-CH_2 antisymmetric stretch	3178	2981	3.1	66.8	0.75	2974	2969	-	$99S_{24}$	0	0
	ν_{25}	β-CH_2 symmetric stretch	3118	2925	44.9	2.8	0.75	2924	2915	-	$99S_{25}$	0	0
	ν_{26}	β-CH_2 deformation	1550	1459	2.2	7.4	0.75	1461	1465	-	$100S_{26}$	0	0
	ν_{27}	γ-CH_2 wag	1324	1258	3.6	0.6	0.75	1288	1258	-	$72S_{27}$	0	0
	ν_{28}	β-CH_2 wag	1291	1226	1.8	3.9	0.75	1220	1233	-	$60S_{28}$, $28S_{30}$	0	0
	ν_{29}	CH out-of-plane bend	1273	1210	2.5	8.7	0.75	~1202	1211	~1216	$38S_{29}$, $25S_{30}$, $20S_{28}$	0	0
	ν_{30}	γ -CH_2 twist	1209	1148	1.0	4.7	0.75	-	-	1141	$10S_{30}$, $32S_{29}$, $29S_{31}$, $10S_{32}$, $10S_{28}$	0	0
	ν_{31}	β-CH_2 twist	1070	1018	12.2	0.5	0.75	~1021	1006	1018	$49S_{31}$, $14S_{35}$, $14S_{30}$,	0	0
	ν_{32}	Ring deformation 1	991	941	4.4	13.2	0.75	~937	947	944	$76S_{32}$	0	0
	ν_{33}	Ring deformation 2	963	925	0.4	0.6	0.75	~912	911	912	$52S_{33}$, $14S_{29}$	0	0
	ν_{34}	SiH out-of-plane bend	844	801	158.8	8.4	0.75	800	798	801	$95S_{34}$	0	0
	ν_{35}	β-CH_2 rock	811	773	0.0	0.0	0.75	~771	-	-	$65S_{35}$, $14S_{33}$, $14S_{30}$	0	0
	ν_{36}	$SiCl_2$ antisymmetric stretch	608	578	138.0	5.0	0.75	~576	~577	580	$92S_{36}$	0	0
	ν_{37}	$SiHCl_2$ Ring bending	297	295	0.0	2.6	0.75	-	~284	-	$55S_{37}$, $33S_{38}$	0	0
	ν_{38}	$SiCl_2$ twist	97	97	0.2	1.0	0.75	-	-	-	$60S_{38}$, $40S_{37}$	0	0
	ν_{39}	$SiCl_2$ rock	39	37	0.1	0.1	0.75	-	-	-	$100S_{39}$	0	0

[a] MP2(full)/6-31G(d) *ab initio* calculations, scaled frequencies, infrared intensities (km/mol), Raman activities ($Å^4$/amu), depolarization ratios and potential energy distributions (P.E.D.s)

[b] MP2(full)/6-31G(d) fixed scaled frequencies with factors of 0.88 for CH and SiH stretches and CH_2 deformations, 1.0 for heavy atom bends, and 0.90 for all other modes.

[c] Contributions less than 10% are omitted.

[d] A and C values in the last two columns are percentage infrared band contours.

Table 3. Observed and calculated[a] frequencies (cm^{-1}) for Ax-g cyclobutyldichlorosilane.

	Vib. No.	Approximate Descriptions	ab initio	fixed scaled[b]	IR int.	Raman act.	dp ratio	IR	Raman		P.E.D.[c]	Band Contours[d]		
								Gas	Liquid	Krypton		A	B	C
	ν_1	γ-CH_2 antisymmetric stretch	3210	3011	26.6	46.5	0.66	2996	2984	2987	$88S_1$, $10S_3$	63	37	-
	ν_2	β-CH_2 antisymmetric stretch	3180	2984	4.1	67.2	0.75	2984	2969	2984	$78S_2$, $19S_3$	22	25	53
	ν_3	β-CH_2 antisymmetric stretch	3175	2978	14.5	65.6	0.67	2974	2969	2968	$69S_3$, $21S_2$	13	85	2
	ν_4	γ-CH_2 symmetric stretch	3143	2948	26.0	124.7	0.11	2954	2948	2948	$97S_4$	70	9	21
	ν_5	β-CH_2 symmetric stretch	3123	2930	16.2	105.7	0.11	2934	2948	2936	$63S_5$, $33S_6$	5	58	37
	ν_6	β-CH_2 symmetric stretch	3116	2924	35.8	59.5	0.10	2924	2915	2924	$66S_6$, $30S_5$	10	5	85
	ν_7	CH stretch	3102	2910	19.7	51.0	0.56	2905	2900	2908	$95S_7$	53	26	21
	ν_8	SiH stretch	2344	2223	131.5	130.7	0.16	2204	2204	2204	$100S_8$	7	2	91
	ν_9	β-CH_2 deformation	1578	1486	0.4	10.0	0.68	-	-	-	$68S_9$, $30S_{10}$	79	0	21
	ν_{10}	γ-CH_2 deformation	1550	1459	3.5	16.4	0.74	1461	1465	-	$67S_{10}$, $30S_9$	4	88	8
	ν_{11}	β-CH_2 deformation	1548	1457	2.9	6.9	0.74	1461	~1465	-	$97S_{11}$	6	3	91
	ν_{12}	β-CH_2 wag	1340	1272	3.4	2.0	0.60	-	1267	-	$55S_{12}$, $25S_{19}$, $13S_{14}$	27	50	23
	ν_{13}	γ-CH_2 wag	1328	1262	3.2	0.6	0.75	1252	1258	-	$72S_{13}$	20	12	68
	ν_{14}	CH in-plane bend	1321	1258	3.1	2.0	0.42	1252	~1258	-	$29S_{14}$, $30S_{12}$, $18S_{19}$,$15S_{23}$	79	21	0
	ν_{15}	β-CH_2 wag	1294	1228	1.8	3.9	0.75	1220	~1233	-	$60S_{15}$, $27S_{20}$	22	11	67
	ν_{16}	γ -CH_2 twist	1274	1211	2.6	8.8	0.75	1202	~1211	1216	$35S_{16}$, $26S_{20}$, $24S_{15}$	13	9	78
	ν_{17}	β-CH_2 twist	1249	1190	3.5	7.9	0.73	1189	1192	1198	$18S_{17}$, $32S_{14}$, $24S_{29}$, $17S_{19}$	87	5	8
	ν_{18}	CH out-of-plane bend	1221	1158	1.4	4.1	0.75	-	-	-	$30S_{18}$, $36S_{16}$	44	6	50
	ν_{19}	β-CH_2 rock	1084	1032	7.5	5.3	0.44	1031	-	1027	$12S_{19}$, $21S_{19}$, $18S_{12}$,	11	20	69
	ν_{20}	β-CH_2 twist	1075	1024	11.7	1.5	0.49	1021	1006	1027	$10S_{20}$, $27S_{18}$, $16S_{19}$, $14S_{17}$	31	55	14

	ν_{21}	Ring breathing	1067	1013	15.2	19.7	0.11	1009	1006	1005	$77S_{21}$, $12S_{19}$	51	46	3
	ν_{22}	Ring deformation 1	1002	951	3.9	13.4	0.75	-	947	950	$78S_{22}$	19	4	77
	ν_{23}	Ring deformation 1	973	937	3.4	0.4	0.23	~937	934	-	$53S_{23}$, $15S_{24}$	95	1	4
	ν_{24}	Ring deformation 2	968	932	6.0	0.4	0.69	~912	911	911	$41S_{24}$, $20S_{23}$, $10S_{16}$	100	-	-
	ν_{25}	Ring deformation 2	889	862	1.7	6.0	0.63	-	857	860	$51S_{25}$, $27S_{29}$	22	74	4
	ν_{26}	SiH out-of-plane bend	844	801	139.6	7.6	0.72	800	798	801	$87S_{26}$	6	94	-
	ν_{27}	SiH in-plane bend	827	787	177.8	7.2	0.72	~791	785	~788	$67S_{27}$	92	5	3
	ν_{28}	β-CH_2 rock	805	765	18.9	0.9	0.67	~767	764	767	$65S_{28}$, $11S_{20}$	93	3	4
	ν_{29}	γ-CH_2 rock	685	664	9.7	1.3	0.69	-	-	-	$35S_{29}$, $40S_{25}$,$15S_{17}$	53	45	2
	ν_{30}	Si-C stretch	662	631	14.0	6.3	0.44	629	630	636	$47S_{30}$, $10S_{32}$, $10S_{27}$	24	74	2
	ν_{31}	$SiCl_2$ antisymmetric stretch	598	569	134.2	5.6	0.74	~568	~560	572	$86S_{31}$	41	59	-
	ν_{32}	$SiCl_2$ symmetric stretch	516	492	46.6	11.4	0.02	~492	492	499	$71S_{32}$	7	24	69
	ν_{33}	$SiHCl_2$ Ring bending	383	376	16.3	1.9	0.73	382	374	374	$38S_{33}$, $26S_{37}$, $14S_{34}$	39	36	25
	ν_{34}	$SiHCl_2$ Ring bending	287	282	0.7	3.6	0.34	-	291	-	$28S_{34}$, $17S_{38}$, $14S_{37}$	39	6	55
	ν_{35}	$SiCl_2$ deformation	190	189	3.3	3.0	0.69	-	189	-	$77S_{35}$	31	15	54
	ν_{36}	Ring puckering	165	163	0.9	0.8	0.54	-	167	-	$74S_{36}$, $12S_{35}$	3	63	34
	ν_{37}	$SiCl_2$ wag	131	129	2.9	1.0	0.70	-	-	-	$29S_{37}$, $50S_{33}$,$17S_{34}$	64	-	36
	ν_{38}	$SiCl_2$ twist	111	110	0.5	1.2	0.75	-	-	-	$62S_{38}$, $24S_{34}$, $11S_{37}$	3	71	26
	ν_{39}	$SiCl_2$ rock	41	39	0.3	0.3	0.75	-	-	-	$95S_{39}$	45	9	46

[a] MP2(full)/6-31G(d) ab initio calculations, scaled frequencies, infrared intensities (km/mol), Raman activities ($Å^4$/amu), depolarization ratios and potential energy distributions (P.E.D.s)

[b] MP2(full)/6-31G(d) fixed scaled frequencies with factors of 0.88 for CH and SiH stretches and CH_2 deformations, 1.0 for heavy atom bends, and 0.90 for all other modes.

[c] Contributions less than 10% are omitted.

[d] A, B and C values in the last two columns are percentage infrared band contours.

Table 4 . Observed and calculated[a] frequencies (cm^{-1}) for Eq-t cyclobutyldichlorosilane.

	Vib. No.	Approximate Descriptions	ab initio	fixed scaled[b]	IR int.	Raman act.	dp ratio	IR	Raman		P.E.D.[c]	Band Contours[d]	
								Gas	Liquid	Krypton		A	C
A′	ν_1	β-CH_2 antisymmetric stretch	3198	3000	36.3	68.2	0.67	2996	2984	2987	$48S_1$, $49S_2$	1	99
	ν_2	γ-CH_2 antisymmetric stretch	3182	2985	8.1	81.0	0.35	2984	2969	2967	$50S_2$, $41S_1$	100	-
	ν_3	CH stretch	3129	2935	11.4	32.3	0.63	2934	2948	2953	$92S_3$,	16	84
	ν_4	γ-CH_2 symmetric stretch	3126	2932	33.8	123.3	0.14	2934	2948	2946	$99S_4$,	100	-
	ν_5	β-CH_2 symmetric stretch	3113	2921	6.7	148.0	0.14	2924	2915	2923	$82S_5$, $10S_1$	8	92
	ν_6	SiH stretch	2343	2222	107.6	95.2	0.12	2204	2204	2208	$100S_6$	-	100
	ν_7	β-CH_2 deformation	1575	1483	1.7	6.3	0.67	-	-	-	$68S_7$, $29S_8$	34	66
	ν_8	γ-CH_2 deformation	1549	1458	4.9	20.0	0.73	1461	~1465	-	$70S_8$, $31S_7$	9	91
	ν_9	β-CH_2 wag	1351	1284	1.5	5.9	0.60	-	-	-	$51S_9$, $24S_{10}$, $15S_{11}$	100	-
	ν_{10}	CH in-plane bend	1301	1237	10.2	4.6	0.75	1234	~1243	1236	$32S_{10}$, $35S_9$, $18S_{11}$	75	25
	ν_{11}	β-CH_2 twist	1266	1205	4.4	5.7	0.75	1202	~1211	1203	$44S_{11}$, $19S_{17}$, $12S_{12}$, $12S_{10}$	93	7
	ν_{12}	β-CH_2 rock	1128	1076	26.8	2.6	0.01	1056	1054	1055	$29S_{12}$, $28S_{13}$	98	2
	ν_{13}	Ring breathing	1055	1002	3.4	14.7	0.16	1000	998	997	$58S_{13}$, $16S_{10}$, $10S_{12}$	2	98
	ν_{14}	Ring deformation 1	959	924	8.6	2.1	0.27	912	911	912	$56S_{14}$, $12S_9$, $10S_{18}$	81	19
	ν_{15}	Ring deformation 2	912	884	2.0	3.8	0.06	876	-	-	$44S_{15}$, $22S_{17}$, $10S_{18}$, $10S_{12}$	-	100
	ν_{16}	SiH in-plane bend	828	787	160.3	9.5	0.73	791	785	787	$92S_{16}$	100	-
	ν_{17}	γ-CH_2 rock	751	718	26.5	3.3	0.10	717	717	719	$35S_{17}$, $20S_{18}$, $14S_{14}$	99	1
	ν_{18}	Si-C stretch	588	569	60.1	1.4	0.61	568	560	570	$20S_{18}$, $36S_{15}$, $16S_{19}$, $14S_{12}$	100	-
	ν_{19}	$SiCl_2$ symmetric stretch	537	514	31.0	8.7	0.08	519	~510	~518	$63S_{19}$, $11S_{23}$	60	40
	ν_{20}	Ring puckering	306	296	2.5	3.3	0.12	-	~284	-	$24S_{20}$, $26S_{23}$, $20S_{18}$, $14S_{19}$	34	66

	ν_{21}	$SiCl_2$ wag	239	234	4.1	3.1	0.31	-	-	-	$29S_{21}$, $34S_{20}$, $26S_{22}$	4	96
	ν_{22}	SiCl2 deformation	161	161	6.5	3.9	0.72	-	159	-	$61S_{22}$, $28S_{21}$	95	5
	ν_{23}	$SiHCl_2$ Ring bending	122	120	10.1	0.4	0.71	-	-	-	$48S_{23}$, $25S_{21}$, $24S_{20}$	-	100
A''	ν_{24}	β-CH_2 antisymmetric stretch	3190	2992	18.6	62.4	0.75	2996	2984	-	$91S_{24}$	-	-
	ν_{25}	β-CH_2 symmetric stretch	3113	2920	27.0	3.6	0.75	2924	2915	-	$91S_{25}$	-	-
	ν_{26}	β-CH_2 deformation	1544	1453	0.9	5.4	0.75	1448	1443	-	$100S_{26}$	-	-
	ν_{27}	γ-CH_2 wag	1321	1255	4.4	3.5	0.75	1248	1258	-	$72S_{27}$	-	-
	ν_{28}	β-CH_2 wag	1305	1238	1.3	0.4	0.75	1234	1243	~1236	$56S_{28}$, $16S_{31}$, $16S_{29}$, $10S_{30}$	-	-
	ν_{29}	CH out-of-plane bend	1279	1214	0.2	7.4	0.75	1202	1211	~1216	$45S_{29}$ $25S_{30}$, $10S_{27}$	-	-
	ν_{30}	γ-CH_2 twist	1235	1173	2.9	6.6	0.75	-	1178	1081	$25S_{30}$, $34S_{28}$, $22S_{31}$	-	-
	ν_{31}	β-CH_2 twist	1041	994	11.8	1.0	0.75	1000	~998	~992	$36S_{31}$, $25S_{33}$, $15S_{32}$	-	-
	ν_{32}	Ring deformation 1	985	936	1.2	10.8	0.75	937	934	935	$48S_{32}$, $28S_{33}$, $11S_{27}$	-	-
	ν_{33}	Ring deformation 2	972	933	4.6	3.4	0.75	937	~934	935	$23S_{33}$, $28S_{32}$, $18S_{31}$, $15S_{29}$	-	-
	ν_{34}	SiH out-of-plane bend	853	810	168.0	9.8	0.75	800	~808	801	$83S_{34}$, $12S_{39}$	-	-
	ν_{35}	β-CH_2 rock	812	772	0.0	0.0	0.75	771	-	-	$74S_{35}$, $12S_{34}$, $11S_{30}$	-	-
	ν_{36}	$SiCl_2$ antisymmetric stretch	607	578	140.0	4.7	0.75	~576	~577	580	$92S_{36}$	-	-
	ν_{37}	$SiHCl_2$ Ring bending	293	290	0.0	3.4	0.75	-	~284	-	$50S_{37}$, $34S_{38}$	-	-
	ν_{38}	$SiCl_2$ twist	85	84	0.2	0.7	0.75	-	-	-	$54S_{38}$, $34S_{37}$, $12S_{39}$	-	-
	ν_{39}	$SiCl_2$ rock	47	45	0.2	0.3	0.75	-	-	-	$86S_{39}$	-	-

[a] MP2(full)/6-31G(d) *ab initio* calculations, scaled frequencies, infrared intensities (km/mol), Raman activities ($Å^4$/amu), depolarization ratios and potential energy distributions (P.E.D.s)

[b] MP2(full)/6-31G(d) fixed scaled frequencies with factors of 0.88 for CH and SiH stretches and CH_2 deformations, 1.0 for heavy atom bends, and 0.90 for all other modes.

[c] Contributions less than 10% are omitted.

[d] A and C values in the last two columns are percentage infrared band contours.

Table 5. Calculated Electronic Energies (Hartree) for the Eq-t and Energy Differences (cm^{-1}) for Eq-g, Ax-t, and Ax-g Forms of cyclobutyldichlorosilane

Method/Basis Set	Eq-t[a]	Energy Difference[b]		
		Eq-g	Ax-t	Ax-g
MP2(full)/6-31G(d)	0.000684	12	164	286
MP2(full)/6-31+G(d)	0.0175112	-6	258	226
MP2(full)/6-31G(d,p)	0.0669021	14	182	331
MP2(full)/6-31+G(d,p)	0.0827558	6	267	259
MP2(full)/6-311G(d,p)	0.456566	57	112	306
MP2(full)/6-311+G(d,p)	0.467003	-35	214	185
MP2(full)/6-311G(2d,2p)	0.5953155	-19	48	90
MP2(full)/6-311+G(2d,2p)	0.6013542	-82	69	26
B3LYP/6-31G(d)	2.2093142	64	266	336
B3LYP/6-31+G(d)	2.2164985	75	280	343
B3LYP/6-31G(d,p)	2.2203848	61	258	331
B3LYP/6-31+G(d,p)	2.2272266	71	271	331
B3LYP/6-311G(d,p)	2.3313051	92	226	308
B3LYP/6-311+G(d,p)	2.3346166	70	235	292
B3LYP/6-311G(2d,2p)	2.3489741	84	207	266
B3LYP/6-311+G(2d,2p)	2.3509751	65	212	251

[a] Energy of conformer is given as -(E + 1365) H.

[b] Energy difference related to the *Eq-t* conformer.

TABLE 6A.Temperature and intensity ratios of the conformational bands Eq-g v. Ax-t of cyclobutyldichlorosilane from the Raman spectra of the liquid krypton solution phase.

T(°C)	1/T ($\times 10^3$ K^{-1})	I_{560}/ I_{944}	I_{703}/ I_{944}
−123.0	7.144	0.7729	1.5208
−133.0	7.692	0.8214	1.5741
−143.0	8.333	0.8921	1.6896
ΔH^a (cm^{-1})		98 ± 45	72 ± 11

[a] Average value: $\Delta H = 85 \pm 10$ cm^{-1} (1.01 ± 0.11 kJ mol^{-1}) with the *Eq-g* conformer the more stable form and the statistical uncertainty (σ) obtained by utilizing all of the data as a single set.

TABLE 6B.Temperature and intensity ratios of the conformational bands Eq-g v. Ax-g of cyclobutyldichlorosilane from the Raman spectra of the liquid krypton solution phase.

T(°C)	1/T ($\times 10^3$ K^{-1})	I_{560}/ I_{636}	I_{703}/ I_{636}
−123.0	7.144	0.7507	1.4772
−133.0	7.692	0.7610	1.4583
−143.0	8.333	0.9341	1.7692
ΔH^a (cm^{-1})		151 ± 69	126 ± 76

[a] Average value: $\Delta H = 138 \pm 42$ cm^{-1} (1.66 ± 0.51 kJ mol^{-1}) with the *Eq-g* conformer the more stable form and the statistical uncertainty (σ) obtained by utilizing all of the data as a single set.

TABLE 6C.Temperature and intensity ratios of the conformational bands Eq-g v. Eq-t of cyclobutyldichlorosilane from the Raman spectra of the liquid krypton solution phase.

T(°C)	1/T ($\times 10^3$ K^{-1})	I_{560}/I_{719}	I_{703}/I_{719}	I_{560}/I_{935}	I_{703}/I_{935}
−123.0	7.144	1.9262	3.7904	0.3340	0.6572
−133.0	7.692	2.5241	4.8370	0.3514	0.6733
−143.0	8.333	2.6899	5.0946	0.3518	0.6662
ΔH^a (cm^{-1})		223 ± 90	197 ± 83	34 ± 21	9 ± 14

[a] Average value: $\Delta H = 116 \pm 43$ cm^{-1} (1.39 ± 0.52 kJ mol^{-1}) with the *Eq-g* conformer the more stable form and the statistical uncertainty (σ) obtained by utilizing all of the data as a single set.

Table 7. Structural parameters[a] (Å and degrees) and rotational constants (MHz) of cyclobutyldichlorosilane.

Structural Parameters	Eq-t	Eq-g	Ax-t	Ax-g
rC_{α}-Si	1.845	1.849	1.849	1.849
rC_{α}-C_{β}	1.559	1.558	1.559	1.560
rC_{α}-$C_{\beta'}$	1.559	1.558	1.559	1.556
rC_{γ}-C_{β}	1.546	1.546	1.546	1.547
rC_{γ}-$C_{\beta'}$	1.546	1.546	1.546	1.547
rSi-Cl_1	2.050	2.050	2.049	2.052
rSi-Cl_2	2.050	2.051	2.049	2.050
rC_{α}-H	1.096	1.098	1.096	1.098
rC_{β}-H_1	1.091	1.092	1.094	1.094
$rC_{\beta'}$-H_1	1.091	1.092	1.094	1.094
rC_{β}-H_2	1.095	1.094	1.094	1.093
$rC_{\beta'}$-H_2	1.095	1.094	1.094	1.093
rC_{γ}-H_1	1.093	1.094	1.093	1.091
rC_{γ}-H_2	1.092	1.093	1.092	1.092
$\angle C_{\alpha}SiCl_1$	109.9	108.9	109.1	111.1
$\angle C_{\alpha}SiCl_2$	109.9	108.8	109.1	108.8
$\angle Cl_1SiCl_2$	109.3	108.7	109.4	108.4
$\angle C_{\beta}C_{\alpha}Si$	118.6	119.8	114.2	116.5
$\angle C_{\beta'}C_{\alpha}Si$	118.6	120.7	114.2	116.5
$\angle C_{\beta'}C_{\alpha}C_{\beta}$	87.3	87.4	87.5	88.0
$\angle C_{\gamma}C_{\beta}C_{\alpha}$	87.8	87.8	88.3	88.7
$\angle C_{\gamma}C_{\beta'}C_{\alpha}$	87.8	87.8	88.3	88.7
$\angle C_{\beta'}C_{\gamma}C_{\beta}$	88.2	88.2	88.4	88.9
$\angle HC_{\alpha}C_{\beta}$	109.7	109.0	116.0	114.9
$\angle HC_{\alpha}C_{\beta'}$	109.7	109.2	116.0	114.8
$\angle HC_{\alpha}Si$	110.7	108.9	107.9	105.8
$\angle HSiC_{\alpha}$	111.9	114.9	114.0	113.3
$\angle H_1C_{\beta}C_{\alpha}$	111.2	117.4	118.8	118.6

$\angle H_1C_{\beta'}C_\alpha$	111.2	117.6	118.8	118.3
$\angle H_1C_\beta C_\gamma$	110.7	118.7	118.3	117.6
$\angle H_1C_{\beta'}C_\gamma$	110.7	118.6	118.3	117.6
$\angle H_2C_\beta C_\alpha$	117.5	111.2	110.1	110.4
$\angle H_2C_{\beta'}C_\alpha$	117.5	111.2	110.1	110.4
$\angle H_2C_\beta C_\gamma$	118.8	110.8	111.3	111.7
$\angle H_2C_{\beta'}C_\gamma$	118.8	110.7	111.3	111.8
$\angle H_1C_\beta H_2$	109.2	109.4	108.7	108.7
$\angle H_1C_{\beta'}H_2$	109.2	109.4	108.7	108.7
$\angle H_1C_\gamma C_\beta$	118.2	110.6	111.1	111.4
$\angle H_1C_\gamma C_{\beta'}$	118.2	110.6	111.1	111.3
$\angle H_2C_\gamma C_\beta$	110.4	118.2	117.9	117.3
$\angle H_2C_\gamma C_{\beta'}$	110.4	118.2	117.9	117.4
$\angle H_1C_\gamma H_2$	109.5	109.5	109.0	109.2
$\tau C_\gamma C_\beta C_{\beta'} C_\alpha$	148.5	148.3	150.9	154.6
$\tau HC_\alpha SiCl$	60.2	63.3	59.7	61.0
A(MHz)	1991.28	1986.82	1925.35	1997.63
B(MHz)	996.60	1030.34	1087.77	1115.48
C(MHz)	698.58	794.54	751.43	862.16

[a] Predicted structural parameters obtained from MP2(full)/6-311+G(d,p) calculation.